Femtosecond multi-filamentation control by mixture of gases: towards synthesised nonlinearity

Benjamín Alonso,[1,3] **Amelle Zaïr,**[1,3,*] **Julio San Román,**[1,3]
Oscar Varela,[2] **and Luis Roso**[2]

[1]*Universidad de Salamanca, Área de Óptica. Departamento de Física Aplicada, Salamanca, E-37008 Salamanca, Spain*
[2]*Centro de Laseres Pulsados Ultracortos Ultraintensos, CLPU E-37008 Salamanca, Spain*
[3]*These authors contributed equally to this work.*
*zair@usal.es

Abstract: We have investigated femtosecond multi-filamentation process in a mixture of gases controlling the concentration of atoms versus molecules in the gas cell. The experimental results show that this control could provide a new freedom degree to deterministic spatial distribution control of the multiple filaments. Our simulation indicates surprisingly that only difference of the gases nonlinearity (referred to as "synthesised nonlinearity") is sufficient to be responsible for this control. This study opens the way to provide few-cycle pulses spatial distributed source for spatially encoded measurements and experiments.

© 2010 Optical Society of America

OCIS codes: (020.0020) Atomic and molecular physics; (320.6629) Supercontinuum generation; (320.7110) Ultrafast non linear optics.

References and links

1. V. I. Bespalov and V. I. Talanov, "Filamentary structure of light beams in nonlinear media," JETP Lett. **3**, 307 (1966).
2. C. P. Hauri, W. Kornelis, F. W. Helbing, A. Heinrich, A. Couairon, A. Mysyrowicz, J. Biegert, and U. Keller, "Generation of intense carrier-envelope phase-locked few-cycle laser pulses through filamentation," App. Phys. B **79**, 673–677 (2004).
3. A. Guandalini, P. Eckle, M. Anscombe, P. Schlup, J. Biegert, and U. Keller, "5.1 fs pulses generated by filamentation and carrier-envelope phase stability analysis," J. Phys. At. Mol. Opt. Phys. **39** S257–S264 (2006).
4. A. Zaïr, A. Guandalini, F. Schapper, M. Holler, J. Biegert, L. Gallmann, U. Keller, A. Couairon, M. Franco, and A. Mysyrowicz, "Spatio-temporal characterization of few-cycle pulses obtained by filamentation," Opt. Express **15**(9), 5394–5404 (2007).
5. O. G. Kosareva, I. N. Murtazin, N. A. Panov, A. B. Savelev, V. P. Kandidov, and S. L. Chin, "Pulse shortening due to filamentation in transparent medium," Laser Phys. Lett. **4**(2), 126–132 (2006).
6. L. Bergé, "Self-compression of 2μ m laser filaments," Opt. Express **16**(26), 21529–21543 (2008).
7. O. D. Mucke, S. Alisauskas, J. A. Verhoef, A. Pugzlys, A. Baltuska, V. Smilgevicius, J. Pocius, L. Giniunas, R. Danielius, and N. Forget, "Self-compression of millijoule 1.5μm pulses," Opt. Lett. **34**(16), 2498–2500 (2009).
8. G. Fibich, S. Eisenmann, B. Ilan, and A. Zigler, "Control of multiple filamention in air," Opt. Lett. **29**(15), 1772 (2004).
9. G. Méchain, A. Couairon, M. Franco, B. Prade, and A. Mysyrowicz, "Organizing Multiple Femtosecond Filaments in Air," Phys. Rev. Lett. **93**, 035003 (2004).
10. A. Dubietis, G. Tamošauskas, G. Fibich, and B. Ilan, "Multiple filamentation induced by input-beam ellipticity," Opt. Lett. **29**(10), 1126 (2004).
11. G. Fibich and B. Ilan, "Multiple Filamentation of Circularly Polarized Beams," Phys. Rev. Lett. **89**(1), 013901 (2002).

#117771 - $15.00 USD Received 9 Jun 2010; revised 14 Jun 2010; accepted 16 Jun 2010; published 7 Jul 2010

12. A. Trisorio and C. P. Hauri, "Control and characterization of multiple circularly polarized femtosecond filaments in argon," Opt. Lett. **32**, 1650–1652 (2007).
13. O. Varela, A. Zaïr, J. San Roman, B. Alonso, I. J. Sola, C. Prieto, and L. Roso, "Above-millijoule supercontinuum generation using polarisation dependent filamentation in atoms and molecules," Opt. Express **17**(5), 3630–3639 (2009).
14. T. Pfeifer, L. Gallmann, M. J. Abel, D. M. Neumark, and S. R. Leone, "Circular phase mask for control and stabilization of single optical filaments," Opt. Lett. **31**(15), 2326–2328 (2006).
15. V. P. Kandidov, N. Akozbek, M. Scalora, O. G. Kosareva, A. V. Nyakk, Q. Luo, S. A. Hosseini, and S. L. Chin, "Towards a control of multiple filamentation by spatial regularization of a high-power femtosecond laser pulse," Appl. Phys. B **80**(2), 267–275 (2005).
16. A. Couairon, H. S. Chakraborty, and M. B. Gaarde, "From single-cycle self-compressed filaments to isolated attosecond pulses in noble gases," Phys. Rev. A **77**, 053814 (2008).
17. A. Couairon and A. Mysyrowicz, "Femtosecond filamentation in transparent media," Phys. Rep. **441**(2–4), 47-189 (2007).
18. J. Wu, H. Cai, H. P. Zeng, and A. Couairon, "Femtosecond filamentation and pulse compression in the wake of molecular alignment more options," Opt. Lett. **33**(22), 2593–2595 (2008).
19. A. S. Wyatt, I. A. Walmsley, G. Stibenz, and G. Steinmeyer, "Sub-10 fs pulse characterization using spatially encoded arrangement for spectral phase interferometry for direct electric field reconstruction," Opt. Lett. **31**(12), 1914–1916 (2006).
20. T. Witting, D. R. Austin, and I. A. Walmsley, "Improved ancilla preparation in spectral shearing interferometry for accurate ultrafast pulse characterization," Opt. Lett. **34**(7), 881–883 (2009).
21. T. Witting, D. R. Austin, and I. A. Walmsley, "Ultrashort pulse characterization by spectral shearing interferometry with spatially chirped ancillae," Opt. Express **17**(21), 18983–18994 (2009).
22. E. Cormier, I. A. Walmsley, E. M. Kosik, A. S. Wyatt, L. Corner, and L. F. DiMauro, "Self-referencing, spectrally, or spatially encoded spectral interferometry for the complete characterization of attosecond electromagnetic pulses," Phys. Rev, Lett. **94**(3), 033905 (2005).
23. Y. Mairesse, D. Zeidler, N. Dudovich, M. Spanner, J. Levesque, D. M. Villeneuve, and P. B. Corkum, "High-order harmonic transient grating spectroscopy in a molecular jet," Phys. Rev. Lett. **100**(14), 143903 (2008).
24. J. A. Perez-Hernandez, D. Hoffmann, A. Zaïr , L. E. Chipperfield, L. Plaja, C. Ruiz, J. P. Marangos, and L. Roso, "Extension of the cut-off in high-harmonic generation using two delayed pulses of the same colour," J. Phys. At. Mol. Opt. Phys. **42**, 13, 134004 (2009).
25. A. Couairon, M. Franco, A. Mysyrowicz, J. Biegert, and U. Keller, "Pulse self-compression to the single-cycle limit by filamentation in a gas with a pressure gradient," Opt. Express **30**(19), 2657–2659 (2005).
26. C. Iaconis and I. A. Walmsley, "Spectral phase interferometry for direct electric-field reconstruction of ultrashort optical pulses," Opt. Lett. **23**, 792–794 (1998).
27. L. Berge, S. Skupin, F. Lederer, G. Mejean, J. Yu, J. Kasparian, E. Salmon, J. P. Wolf, M. Rodriguez, L. Wöste, R. Bourayou, and R. Sauerbrey, "Multiple Filamentation of Terawatt Laser Pulses in Air," Phys. Rev. Lett. **92**, 225002 (2004).

1. Introduction

In filamentation experiments involving the propagation of high-power ultrashort laser pulses in transparent media, it is now well-known that when the input beam power exceeds several times the critical power for self-focusing (P_{cr}), the transverse spatial beam profile breaks up into multiple filaments (MF). For high input powers corresponding to hundred's times P_{cr}, it has been demonstrated theoretically by Bespalov and Talanov [1] that MF originate from initial random noise in the input beam profile. For input powers of few P_{cr}, commonly used now for post-compression of IR laser pulses [2–5] and possibly extendible to mid-IR laser pulse [6, 7], this initial random noise induces first a collaps as a single filament (SF) and after small propagation distance could break up into MF. In this regime the random noise induces only stochastic distribution of the transverse spatial beam profile that depends on each laser shot, minimising possible applications of such laser beam distribution. However, since many years, G. Fibich, B. Ilan and coworkers [8] as well as A. Couairon and co-workers [9] addressed the question of modelling the MF in a deterministic regime and demonstrated theoretically its origin as breakup of initial beam cylindrical symmetry resulting from vectorial effect. This can be achieved experimentally modifying the characteristics of the input beam using super gaussian and elliptical spatial profiles [10], circular polarisation [11–13], astigmatic beams [8]

#117771 - $15.00 USD Received 9 Jun 2010; revised 14 Jun 2010; accepted 16 Jun 2010; published 7 Jul 2010
(C) 2010 OSA

or amplitude and phase masks [14, 15]. In our recent work [13] we notice in linear polarisation a clear difference between the atomic and the molecular MF transverse spatial distribution. To explain the spatial distribution difference observed, we proposed an initial hypothesis based on additionnal anisotropy in the molecular compared to the atomic response. To clarify this point and to investigate a new method for deterministic spatial MF control, we present in this article a study on the MF spatial distribution controlling the concentration of mixture of gases composed of atoms (Argon) and molecules (Nitrogen) with equivalent ionisation level (I_p) to undergo the same ionisation process , different nonlinear index ($n_2(N_2) = 2.3 \times 10^{-19} cm^2/W$; $n_2(Ar) = 1.74 \times 10^{-19} cm^2/W$) and ionisation cross section (at 800 nm and for multiphoton ionisation K=11, $\sigma(N_2) = 6.31 \times 10^{-140} s^{-1} cm^{2K} W^K$; $\sigma(Ar) = 6.0 \times 10^{-140} s^{-1} cm^{2K} W^K$ [16–18]) that lead to comparable electron density ρ. This choice will allow us to identify if the nonlinearity could be responsible for the different MF distribution observed [13].

In this article we demonstrate a control on double femtosecond filamentation spatial distribution providing a new manner to control deterministic MF. The measurement of super continuum from pulses propagating through each filaments channel shows the capability of deterministic MF spatial distribution controlled by gas mixture to provide source of few-cycle pulses spatially distributed. Such source could be applied to spatially encoded measurements such as SEA-SPIDER [19–21] and its XUV version using High-order harmonic generation, XUV-SEA-SPIDER [22]. This source will also be quite useful to explore new High-order harmonic schemes such as transient gratings [23] or method for cut-off frequency extension using two few-cycle laser pulses of same colour [24].

2. Experiment and results

We defined for our experiment the concentration of gas mixture composed of argon atoms and nitrogen molecules as the ratio of atomic and molecular moles in the interaction volume. For its description we considered equation of state following the Van der Waals law for both gases species (Van der Waals constants specific of each gas are used). The Van der Waals equation can be analytically inverted thus obtaining the number of moles as a function of the gas pressure of each species used. Controlling the partial pressures of each gas in our set-up allowed to control the concentration of atom versus molecule applying the Dalton's law for the total pressure definition. The Dalton's law is used considering that in our experiment no pressure gradient has been used [25] but static pressure in the cell target so that the total pressure is uniform over the propagation length with local thermal equilibrium. We generate filaments using a few-mJ linearly polarised 35 fs IR pulses source at a repetition rate of 10 Hz from our laser system (Amplitude Inc.) that provides average power up to the TW level. The laser beam is focused with a spherical silver mirror (Radius of Curvature ROC -3000 mm) into a gas cell of 2 m long filled with the mixture of gases and the output beam is then collimated. A set of chirped mirrors is used to compress the output pulse over the large bandwidth generated through self-phase modulation along the filament. The gas cell is filled with a mixture of two gases species: argon (atomic) and nitrogen (molecular) at different partial pressures. The concentration of the gas mixture is gradually changed from 100 % nitrogen (gas target composed only of molecules) to 100% argon (gas target without molecules). For each measurement, the cell is filled at the partial pressures needed. During all the measurement the total pressure in the cell is maintained. The cell is then pumped in between each partial pressure setting. As a reference, we first generate a SF using an input energy of 4.8 mJ and a total pressure of 980 mbar in pure argon cell target. Then, by increasing the pressure in the cell up to 1400 mbar, we induce double filaments transverse spatial distribution in pure argon cell target. In both experiments, we study the spatial profile evolution with the gas concentration. We also measured the spectral distribution and the output energy in a spatially selected child-filament, as explained below, to check that a

#117771 - $15.00 USD Received 9 Jun 2010; revised 14 Jun 2010; accepted 16 Jun 2010; published 7 Jul 2010
(C) 2010 OSA

continuum was generated and to compare energy under each configuration for a given child-filament.

In the SF regime as shown in the Fig. 1(a), the spatial distribution is not dramatically affected by the concentration of the gas target. This measurement is taken as reference since the filament formation remains unchanged and is compared to the behaviour of MF with the concentration. The SF mode presents a broad spectra corresponding to a 13 fs pulse (compress factor of ~ 3) measured by SPIDER [26] containing $\sim 600\mu J$ for the pure nitrogen target case (inner core selection [4]). The evolution of the spectrum in the SF inner core with respect to the concentration of gas is shown in Fig. 2(a). For each concentration the output energy as well as the central frequency (centroid of the spectral distribution) has been measured and listed in the figure. The spectrum is getting slightly narrower from the pure molecular to the pure atomic target due to different nonlinearity and Raman emission in the molecular case and it follow the increase of energy throughput. Indeed, the diameter of the output selection is kept to 3 mm (inner core selection). Figure 1(b) presents the MF spatial distribution dependence with the concentration

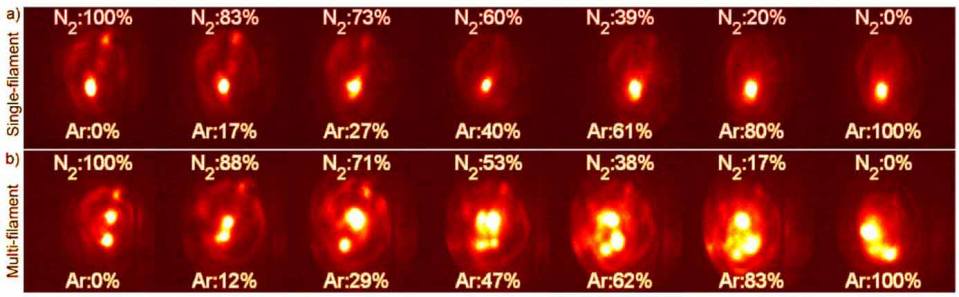

Fig. 1. Dependence of single filament (a) and multi-filament (b) spatial distribution with concentration of argon/nitrogen in the cell target. The single filament case is unchanged by the target concentration and is taken as reference in this experiment. The multi-filamentation distribution exhibits a clear dependence with the concentration of gas and highlight the possibility to use this new degree of freedom for controlling the deterministic position of the child-filaments produced.

of molecules/ atoms in the cell target. In the case of pure nitrogen target and pure argon target the orientation of the double filamentation is quasi-symmetrical in the transverse plane and has been already observed in our previous work [13] where we also noticed that this particular distribution was independent on the polarisation state of the input beam. In our experiment the MF orientation in the pure argon cell target, is determined by an elliptical spatial beam profile that breaks the cylindrical symmetry in the transverse plane to the propagation axis. The MF profiles are shown in Fig. 1b, exhibiting a double filament distribution that is clearly dependent on the concentration of the gas target. Note that we decided to reduce our study to double filament which corresponds to the ideal source for spatially encoded interferometry measurements. Indeed while a double filament is generated in pure argon target to a pure nitrogen target, the double filamentation structure rotates around the propagation axis in such way that the axis of the double filamentation distribution is quasi-symmetrical in the transverse plane from pure nitrogen cell target to pure argon one. Varying the ratio of gases while maintaining the total pressure fixed, we are able to track the evolution of the multi-filamentation from pure nitrogen to pure argon gas target. In a first step, when the nitrogen ratio is above 70%, the nitrogen still carries the filamentation dynamics and the double filamentation axis slightly change its orientation but remains close to the pure nitrogen one. One can notice the particular case of a cell filled with same amount of atoms and molecules (53%/47%) where four child-filaments are

#117771 - $15.00 USD Received 9 Jun 2010; revised 14 Jun 2010; accepted 16 Jun 2010; published 7 Jul 2010
(C) 2010 OSA

present. This particular case illustrates the transition from one set of double filaments to the other one. While passing the barrier of 50% of argon in the target, the double filament distribution changes dramatically and switch to the second set of filament present in the MF pattern in the 53%/47% case. This rotation of MF with the concentration of the target is reproducible shot to shot and so results in a deterministic distribution observed here. The filamentation output characterisation is completed with the measurement of the output energy and spectra in each child-filamentation. For this purpose, a suitable spatial selection of the child-filament is done, according to the criteria of having stable spatial mode and unchanged spectrum in the whole selection. In the multi-filamentation experiment, the measurements shown were taken for the upper filament [the common one, see Fig. 1(b)] because it is preserved along the different gas mixtures. The spectrum of this common filament of MF regime for different concentration of gases is shown in Fig. 2(b). The transition for pure nitrogen to pure argon is also tracked in the evolution of the spectrum. The longer wavelengths tail generation disappears when decreasing the partial pressure of nitrogen, whereas the shorter wavelengths broad tail is more modulated when argon is more plentiful. The central wavelength and the energy of the common filament are shown inside the figure for the different concentrations. The energy of this filament hardly varies. However, the central wavelength calculated as the gravity centre of the spectrum experience slight blue-shift towards pure argon case, due to the absence of Raman emission for the atomic target case.

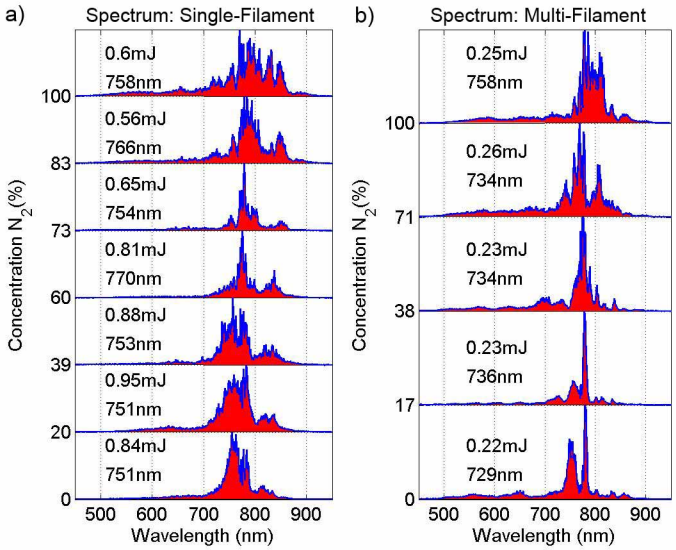

Fig. 2. Spectral distribution for the single filament (a) and for one of the child-filament within the multifilament regime (b), as a function of the gas concentration.

3. Model and discussion

In our experiment we first checked that the rotation of the linearly polarised input pulse did not change the double filament orientation neither in argon nor in nitrogen. So any asymmetries depending on the polarisation (such as ionisation or ultra-fast molecular alignment) could not explain the change on the axis between the argon experiment and the nitrogen experiment. The experiment has been performed under same laser conditions (same pulse duration, same input laser beam profile). Our hypothesis to explain the observations consists of considering that

#117771 - $15.00 USD Received 9 Jun 2010; revised 14 Jun 2010; accepted 16 Jun 2010; published 7 Jul 2010
(C) 2010 OSA

the filamentation process begins at different propagation distances for the argon than for the nitrogen due to their different nonlinearity. As we are dealing with elliptic spatial beam profiles, the spatial profile along the propagation will change which could lead, depending on the starting point of the filamentation process for each gas, to different multi-filamentation patterns. To further understand this behaviour, we have implemented numerical simulations of the multi-filamentation nonlinear propagation using a elliptical profile for the input beam. In this model, we take into account the diffraction, the instantaneous and retarded Kerr effect in the molecular case, the plasma defocusing and the multi-photon absorption. Obviously, in our experiments the Raman effect (retarded Kerr) will be only present for the molecular gas, which enlarges the nonlinear differences between both gases. Since the propagation lacks cylindrical symmetry, we have used the temporally averaged model proposed by L. Bergé, S. Skupin and co-workers, shown below, where the temporal coordinate disappears simplifying a lot the computing time [27].

$$i\partial_z\psi + \frac{1}{2k_0}\nabla_\perp^2\psi + \alpha k_0 n_2|\psi|^2\psi - \gamma|\psi|^{2K}\psi + i\nu|\psi|^{2K-1}\psi = 0 \tag{1}$$

where ψ denotes the pulse envelope without the temporal dependence, which has been averaged [27], k_0 the wave number corresponding to the central wavelength, t_p the half-width pulse duration, n_2 the nonlinear refraction index, τ_K accounts for the retarded Kerr effect in the molecule (Raman) which is taken obviously to 0 for the atom case, T the temporal length of the main structure that emerges from the pulse propagation through the filament (here we assume the same duration $t_p/2$, assuming that the final pulse keeps the same order of magnitude meaning some fraction of the input pulse duration t_p), $\alpha = \frac{1-x_{DK}}{\sqrt{2}} + \frac{x_{DK}D(t_p)}{2\tau_K}$ with $D(t_p) = \int_{-\infty}^{+\infty} exp[\frac{T^2}{8\tau_K^2} - \frac{u}{\tau_K} - \frac{2u^2}{T^2}][erf(\frac{\sqrt{2}u}{T} - \frac{T}{\sqrt{8}\tau_K} + 1)]du$, denotes a nonlinear coefficient that appears under the temporal average, $\gamma = k_0\sigma_K\rho\sqrt{\frac{\pi}{8K}}\frac{T}{2\rho_c}$ the coefficient associated to the plasma defocusing (which density ρ is calculated using the Drude model and critical one ρ_c), K is the number of photons involved in the multiphoton ionisation process and σ_K the related coefficient, $\nu = \frac{\beta^K}{2\sqrt{K}}$ the coefficient associated to the multiphoton absorption. The parameter x_{DK} is taken equal to 0 for the atom where the nonlinearity is then purely electronic and 0.5 for the molecule where the Raman emission is then accounted through $D(t_p)$ (for all others parameters see caption Fig. 3). We have studied the propagation of the beam for argon and nitrogen using the same elliptical input beam. The parameters used coincide with the experimental conditions (3 mm FWHM diameter, 800 nm central wavelength and $t_p = 34fs$ FWHM duration, focused by 1.5 m focal length lens in 1 atm pressure of gas, spatial distribution calculated after $z = 2m$ propagation). The input energy used for the calculation (2.5 mJ in argon and in nitrogen), is chosen the same in both cases to lead to multiple filamentation regime. In Fig. 3, these conditions lead to two child-filaments in argon and quasi four in nitrogen due to different Kerr effect contribution. However, the multi-filamentation distribution exhibits a clear dependence with the gas species used: the two child-filaments visible in the argon target appear as four child-filaments in nitrogen with two main ones oriented at 90° of the orientation of the argon child-filaments.

By looking at the distribution of the child-filaments over the propagation axis (scenario described in Media 1) , we notice indeed that in the argon case the MF formation appears before the geometrical focus. The model shows in this case that almost five small filaments are generated in that early stage of the nonlinear propagation region. Further away the central filament disappears, and when reaching the end of the tube, after two meters of propagation [see Fig. 3(a)], two of the four filaments keeps almost all the energy, being these aligned parallel to the elliptical spatial distribution of the beam at the focus when it is propagated linearly. In the

#117771 - $15.00 USD Received 9 Jun 2010; revised 14 Jun 2010; accepted 16 Jun 2010; published 7 Jul 2010
(C) 2010 OSA

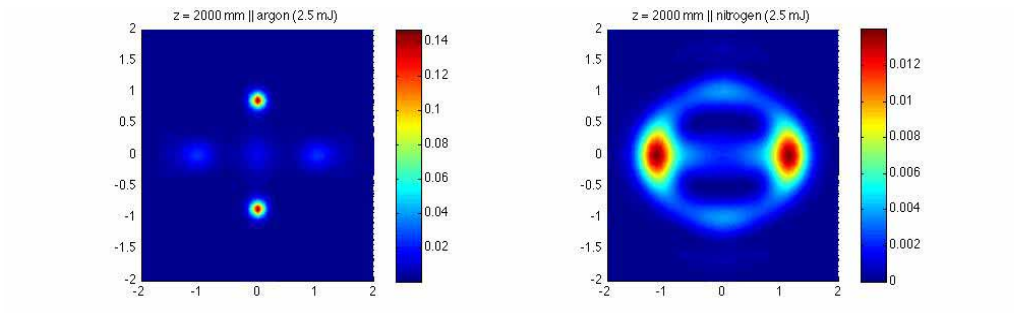

Fig. 3. (Media 1) Calculated dependence of multiple filaments spatial distribution in pure (concentration of 100 %) argon (a) and nitrogen (b)target at the output of the cell target (propagation over z=2 m). The multi-filamentation distribution exhibits a clear dependence with the gas species used. The following values have been taken for the simulation: $K = 11$, $\sigma_K = 6.31 \times 10^{-140} s^{-1} cm^{22} W^{-11}$, $n_2 = 2.3 \times 10^{19} cm^2/W$ for N_2 and $\sigma_K = 6.0 \times 10^{-140} s^{-1} cm^{22} W^{-11}$, $n_2 = 1.74 \times 10^{19} cm^2/W$ for Ar, $\tau_K = 70 fs$, $\rho = 2.5 \times 10^{19} cm^{-3}$, $\rho_c = 1.8 \times 10^{21} cm^{-3}$ [16–18].

case of nitrogen, a different behaviour is observed: the MF formation occurs around the geometrical focus, where three filaments are generated, aligned perpendicular to the linear spatial distribution of the beam at the focus. After the propagation along the two meters cell the central filament disappears giving all its energy to the other two, which are the two filaments observed at the end of the cell [see Fig. 3(b)].

This model affords qualitatively the experimental observation and suggests that the double filament control originates from the different nonlinear propagation in the two gases used. Off course, a complete study accounting "real" gases mixture could help identifying within the nonlinearity which contribution (electronic, Raman or both) is related to our observation. However, it is clear here that mixture of two gases with different n_2 provides a "synthesised nonlinearity" which leads to a control of the MF. This synthesised nonlinearity provides also new type of medium with adaptive nonlinear response, which will be of great interest to study moreover.

4. Conclusion

In this work, we have studied for the first time to our knowledge the implication of gas mixture with equivalent ionisation level to control deterministic multi-filamentation formation. We demonstrate this control on double femtosecond filamentation spatial distribution providing a new method for the control of deterministic MF. Our simulation shows the implication of the synthesised nonlinearity in the control process and suggest that only a difference of nonlinear propagation between the two gases used, is necessary to induce such control. The synthesised nonlinearity obtained is not only of great interest for the multi-filamentation control but it also provides new types of medium with new nonlinearities that cannot be obtained in pure medium. The measurement of supercontinuum from pulses propagating through each child-filaments offers the possibility to use this new degree of freedom for providing source of few-cycle pulses spatially distributed, useful for sources characterisation from IR to XUV [19–22] and secondary sources for high-order harmonic generation [23, 24].

Acknowledgements

We acknowledge support from Spanish Ministerio de Ciencia e Innovación through the Consolider Program SAUUL (CSD2007-00013), Research project FIS2009-09522 and from Junta

de Castilla y León through the Program for Groups of Excellence (GR27). We also acknowledge support from the Centro de Laseres Pulsados, CLPU, Salamanca, Spain. The research work of Benjamin Alonso is supported by the MICINN through the Formación de Profesorado Universitario grant program. Dr. Amelle Zaïr thanks Dr. Roland Guichard , Dr. Stefan Skupin and Dr. Luis Plaja for fruitfull discussions.